



Cite this: *Dalton Trans.*, 2016, **45**, 1225

Mechanical mixtures of metal oxides and phosphorus pentoxide as novel precursors for the synthesis of transition-metal phosphides†

Lijuan Guo,^a Yu Zhao^b and Zhiwei Yao^{*b}

This study presents a new type of precursor, mechanical mixtures of metal oxides (MOs) and phosphorus pentoxide (P₂O₅) are used to synthesize Ni₂P, Co₂P and MoP phosphides by the H₂ reduction method. In addition, this is first report of common solid-state P₂O₅ being used as a P source for the synthesis of metal phosphides. The traditional precursors are usually prepared *via* a complicated preparation procedure involving dissolution, drying and calcination steps. However, these novel MOs/P₂O₅ precursors can be obtained only by simple mechanical mixing of the starting materials. Furthermore, unlike the direct transformation from amorphous phases to phosphides, various specific intermediates were involved in the transformation from MOs/P₂O₅ to phosphides. It is worthy to note that the dispersions of Ni₂P, Co₂P and MoP obtained from MOs/P₂O₅ precursors were superior to those of the corresponding phosphides prepared from the abovementioned traditional precursors. It is suggested that the morphology of the as-prepared metal phosphides might be inherited from the corresponding MOs. Based on the results of XRD, XPS, SEM and TEM, the formation pathway of phosphides can be defined as MOs/P₂O₅ precursors → complex intermediates (metals, metal phosphates and metal oxide-phosphates) → metal phosphides.

Received 19th September 2015,
Accepted 1st December 2015

DOI: 10.1039/c5dt03671b

www.rsc.org/dalton

1. Introduction

Transition metal phosphides have attracted much attention in the past 20 years, owing to their unique properties and potential applications in the fields of photonics, electronics, magnetism, and catalysis.^{1–4} In particular, they have been used as excellent catalysts in many reactions such as hydrogenation and hydrotreating,^{5–8} H₂ evolution reaction,^{2,9,10} N₂H₄ decomposition,^{11–13} and NO reduction.¹⁴ It is worthy to note that Ni₂P phosphide is reported to be a very efficient hydrodesulfurization catalyst in terms of both activity and resistance to poisoning.^{15,16} Thus, extensive effort has been focused on developing methods for synthesizing metal phosphides.

There are a variety of methods reported regarding the preparation of metal phosphides,¹⁷ including direct reduction of phosphate in H₂ or H₂ plasma,^{15,18,19} reaction of metal/metal oxide with PH₃,²⁰ solid-state reaction methods using white or red phosphorus,^{21,22} decomposition of high-boiling point tri-*n*-octylphosphine (TOP) or P(SiMe₃)₃,^{23–27} decompo-

sition of single-source precursors in solution,²⁸ microwave or solvothermal synthesis,^{29,30} and chemical vapor deposition.³¹ The main phosphorus sources in these syntheses can be divided into four groups:¹⁷ (i) tri-*n*-octylphosphine (TOP), alkyl- and aryl-phosphines, (ii) elemental white phosphorus and red phosphorus, (iii) P(SiMe₃)₃ and single-source precursors and (iv) other phosphorus sources such as diammonium/sodium hydrogen phosphate, PH₃, and PCl₃. However, most of these phosphorus sources (TOP, PH₃, P(SiMe₃)₃ and P₄) are highly toxic, and cannot afford the current requirements for green chemistry. In general, diammonium hydrogen phosphate ((NH₄)₂HPO₄) was recognized as an environmentally-friendly phosphorus source for the preparation of phosphide catalysts *via* the H₂ temperature-programmed reduction (H₂-TPR) method.¹⁹ Nevertheless, there were two shortcomings on the use of (NH₄)₂HPO₄ as a phosphorus source in this synthetic route. On the one hand, the preparation of precursors for phosphides involved complicated steps as follows:³² the dissolution of (NH₄)₂HPO₄ and metal salts, and subsequent drying and calcination. On the other hand, the as-prepared precursors and resulting intermediates from them were almost always amorphous so their structural phases were difficult to determine. Therefore, the pathway of reduction for this type of precursor into metal phosphides has not been clarified completely yet. The reduction process was still represented by the following equation: $z\text{MO}_x + \text{PO}_y + (nx + y)\text{H}_2 \rightarrow \text{M}_z\text{P} + (nx + y)\text{H}_2\text{O}$.^{18,19,33,34}

^aCollege of Basic Medical Sciences, Changsha Medical University, Changsha, 410219, P.R. China

^bCollege of Chemistry, Chemical Engineering and Environmental Engineering, Liaoning Shihua University, Fushun, 113001, P.R. China.

E-mail: mezhwei@163.com

†Electronic supplementary information (ESI) available. See DOI: 10.1039/c5dt03671b

In this study, we described a modified H₂ reduction method for synthesizing metal phosphides, in which the precursors for phosphides were obtained simply by mechanical mixing of metal oxides (MOs) and P₂O₅. Moreover, to our knowledge, this is the first time that this type of common P₂O₅ has been used as a phosphorus source for metal phosphide synthesis. The pathway for the transformations of MOs/P₂O₅ mixtures into phosphides can be proposed by combining XRD, XPS, SEM and TEM studies.

2. Experimental

2.1 Sample preparation

In a typical experiment, transition metal phosphides were prepared in two steps. First, the precursors for Ni₂P, Co₂P and MoP were prepared by the mechanical mixing method through co-grinding P₂O₅ and the corresponding metal oxides (MOs) with stoichiometric M/P ratios. The MOs were obtained by the calcination of metal salts (Ni(NO₃)₂·6H₂O, Co(NO₃)₂·6H₂O) and (NH₄)₆Mo₇O₂₄·4H₂O) at 500 °C for 3 h in a muffle furnace. The precursors were heated in a quartz reactor under a flow of H₂ (50 ml min⁻¹). The temperature was increased linearly at a rate of 10 °C min⁻¹ and then maintained at 650 °C (for Ni₂P and Co₂P) or 750 °C (for MoP) for 1 h, followed by cooling to room temperature (RT) under H₂ flow, and then passivated at RT in a stream of 0.5% O₂/Ar for 2 h. To clarify the formation process, the effect of reduction temperature was investigated. The precursors were reduced from 400 to 650 °C for Ni₂P, 500 to 650 °C for Co₂P, and 500 to 750 °C for MoP. The resultant products were designated as Ni-H₂-400, -500, -600 and -650, Co-H₂-500, -600 and -650, and Mo-H₂-500, -650 and -750. In addition, these precursors were also heated in Ar flow (50 ml min⁻¹) at 500 °C, and the resulting samples were designated as Ni-Ar-500, Co-Ar-500 and Mo-Ar-500.

2.2 Sample characterizations

X-Ray diffraction (XRD) analysis of the samples was performed by a X'Pert Pro MPD diffractometer equipped with a Cu K α source. X-ray photoelectron spectroscopy (XPS) study was conducted by a Kratos Axis ultra (DLD) equipped with an Al K α X-ray source. Charging effects were corrected on the basis of adventitious carbon (284.6 eV) referencing. The morphology of the samples was characterized by scanning electron microscopy (SEM, Hitachi S-4800) and transmission electron microscopy (TEM, Philips Tecna 10).

3. Results and discussion

3.1 Microstructural characterization

Fig. 1 shows the XRD patterns of metal phosphides synthesized by reduction of mixtures of MOs and P₂O₅ in H₂. The peak positions were consistent with previous findings for the synthesis of Ni₂P, Co₂P and MoP. There were no diffraction peaks that can be assigned to metal phosphates, metal oxides,

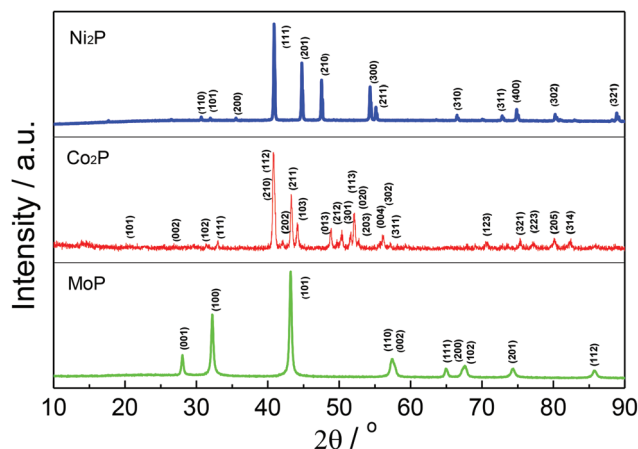


Fig. 1 XRD patterns of Ni₂P, Co₂P and MoP synthesized from their MOs/P₂O₅ precursors.

metal oxide-phosphates or other phosphide phases, indicating that the as-prepared Ni₂P, Co₂P and MoP materials were phase-pure. In addition, the results indicated that the simple mechanical mixing method was effective enough to ensure a uniform distribution of MOs and P₂O₅.

To further confirm the formation of Ni₂P, Co₂P and MoP phosphides, subsequent XPS analysis was conducted. Fig. 2 shows the XPS spectra of the P 2p, Ni 2p, Co 2p, Mo 3d and O 1s regions for the phosphides prepared from MOs/P₂O₅ precursors. On the basis of curve fitting, the binding energies of P 2p_{3/2}, Ni 2p_{3/2}, Co 2p_{3/2}, Mo 3d_{5/2} and O 1s as well as the surface element concentrations and distribution of these corresponding species are listed in Tables 1 and 2. Because the as-prepared metal phosphides were usually passivated before exposure to air, the surface regions of all the samples should be dominated by oxidized species and the underlying phosphided species.^{35,36} In the case of the P 2p XPS spectra, two P 2p peaks were observed at 129.2–129.4 and 133.1–133.5 eV, which were attributed to the phosphided species (P^{δ-}) and oxidized species (P^{δ+}).³⁷ The results demonstrated the formation of phosphides of Ni, Co and Mo. For the Ni₂P sample, two peaks were observed at 853.2 and 856.4 eV in the Ni 2p_{3/2} region, corresponding to the Ni^{δ+} species in Ni₂P and Ni²⁺.³⁸ For Co₂P sample, one peak was observed at 781.2 eV in the Co 2p_{3/2} region, which was assigned to Co²⁺,³⁹ however, no peak was visible at around 778.3 eV for Co^{δ+} species⁴⁰ in Co₂P. This was probably due to the fact that the Co^{δ+} species was so low in concentration that its corresponding peak area was overshadowed by that of Co²⁺ species. This suggested that there was a thicker passivation layer on the surface of the Co₂P sample. For the MoP sample, the Mo 3d_{5/2} peaks at 228.1, 229.3 and 232.4 eV were ascribed to the Mo^{δ+} species in MoP, Mo⁴⁺ and Mo⁶⁺, respectively.⁴⁰ The O 1s XPS spectra consisted of two peaks at 533.1–533.4 and 531.4–531.9 eV, which were typically assigned to the bridging oxygen linking two phosphate groups together (P–O–P) and the non-bridging oxygen terminating the phosphates (–PO_x), respectively.⁴¹ The results

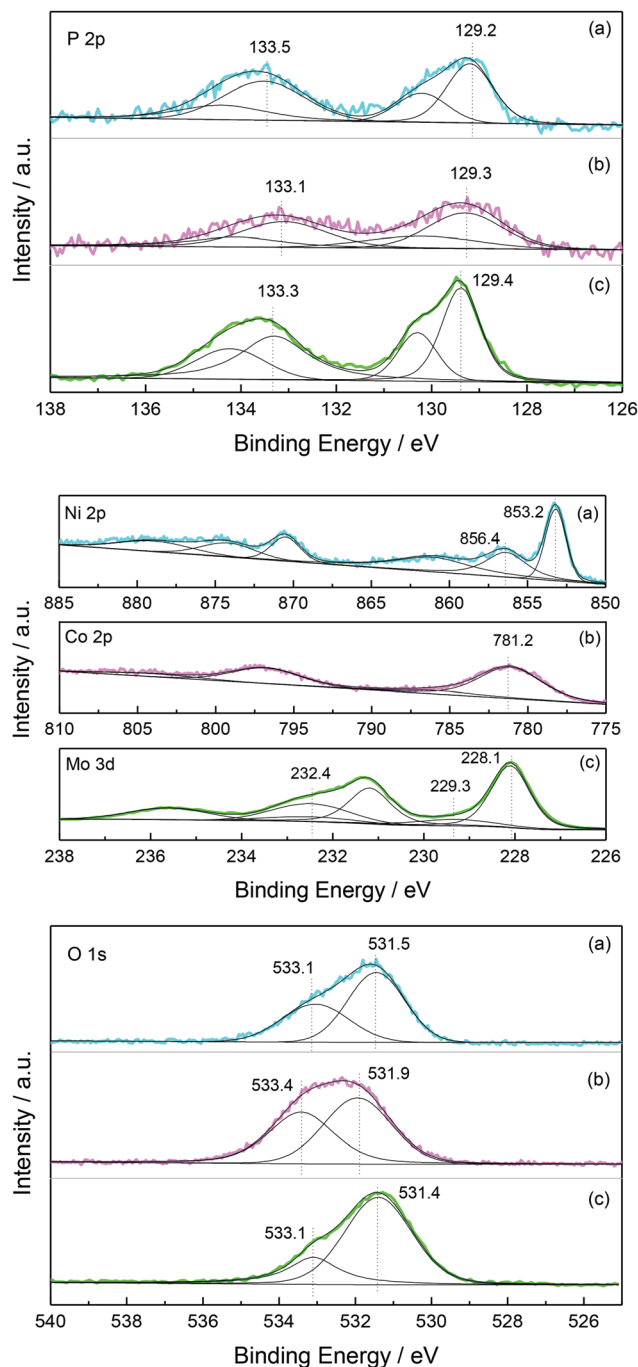


Fig. 2 XPS spectra of P 2p, Ni 2p, Co 2p, Mo 3d and O 1s in (a) Ni₂P, (b) Co₂P and (c) MoP.

Table 1 Surface element concentrations as determined by XPS

Sample	Element concentration (at%)			
	C 1s	O 1s	P 2p	Ni 2p, Co 2p, Mo 3d
Ni ₂ P	35.03	32.99	14.00	17.98
Co ₂ P	63.09	23.81	7.66	5.44
MoP	45.53	34.75	8.33	11.39

Table 2 Binding energies for species on the surfaces of the Ni₂P, Co₂P and MoP samples obtained in this study

Sample	Binding energy (eV)					
	Ni 2p _{3/2}		P 2p _{3/2}		O 1s	
	Ni ^{δ+}	Ni ²⁺	p ^{δ-}	p ⁵⁺	P-O-P	-PO _x
Ni ₂ P	853.2	856.4	129.2	133.5	533.1	531.5
	Co 2p _{3/2}		P 2p _{3/2}		O 1s	
	Co ^{δ+}	Co ²⁺	p ^{δ-}	p ⁵⁺	P-O-P	-PO _x
Co ₂ P	—	781.2	129.3	133.1	533.4	531.9
	Mo 3d _{5/2}		P 2p _{3/2}		O 1s	
	Mo ^{δ+}	Mo ^{4+/Mo⁶⁺}	p ^{δ-}	p ⁵⁺	P-O-P	-PO _x
MoP	228.1	229.3/232.4	129.4	133.3	533.1	531.4

indicated that the passivation-induced oxidized species were metal phosphates rather than metal oxides because no peaks were observed at about 529.7, 530.2 and 530.7 eV for NiO, CoO and MoO_x, respectively.^{42–44}

Finally, the morphologies of Ni₂P, Co₂P and MoP (hereafter denoted as S-Ni₂P, S-Co₂P and S-MoP, respectively) obtained from solid mixtures (MOs and P₂O₅) were characterized by SEM and TEM. For the sake of comparison, Ni₂P, Co₂P and MoP (hereafter denoted as L-Ni₂P, L-Co₂P and L-MoP, respectively) were prepared from traditional raw materials (liquid mixtures of metal salts and (NH₄)₂HPO₄) described elsewhere,³⁸ and their morphologies were also investigated by means of SEM (see ESI†). It can be observed from SEM images (Fig. 3a–c) that the morphologies of S-Ni₂P, S-Co₂P and S-MoP were similar and they were composed of dispersed particles. It was noteworthy that the dispersions of these particles were on the nanoscale for the Co₂P and MoP samples. These results were in good agreement with the observed TEM images (Fig. 4). In addition, the HRTEM images clearly showed that the measured spacings between lattice fringes of 0.22, 0.43 and 0.32 nm were consistent with the *d*-spacings of the (111) plane of Ni₂P (card no. 65-1989), the (101) plane of Co₂P (card no. 32-0306) and the (001) plane of MoP (card no. 65-6487), respectively. On the contrary, the L-Ni₂P and L-Co₂P samples consisted of particles with serious conglomeration and the L-MoP sample consisted of submicrometer-sized MoP thin sheets (see Fig. S1a–c†), which was in accord with the SEM results reported by others.^{38,45–47} It was reported that the morphology of metal phosphides depended highly on the used metal oxide precursors.^{48,49} Therefore, the SEM images of these MOs (NiO, Co₃O₄ and MoO₃) used in the study were shown in Fig. S2a–c.† It was found that the morphologies of S-Ni₂P, S-Co₂P and S-MoP samples were indeed similar to those of corresponding MOs. The results suggested that the morphology of the metal phosphides obtained using MOs/P₂O₅ mixtures as precursors might be controlled by adjusting the morphology of the MOs. Further investigations about this aspect are in progress.

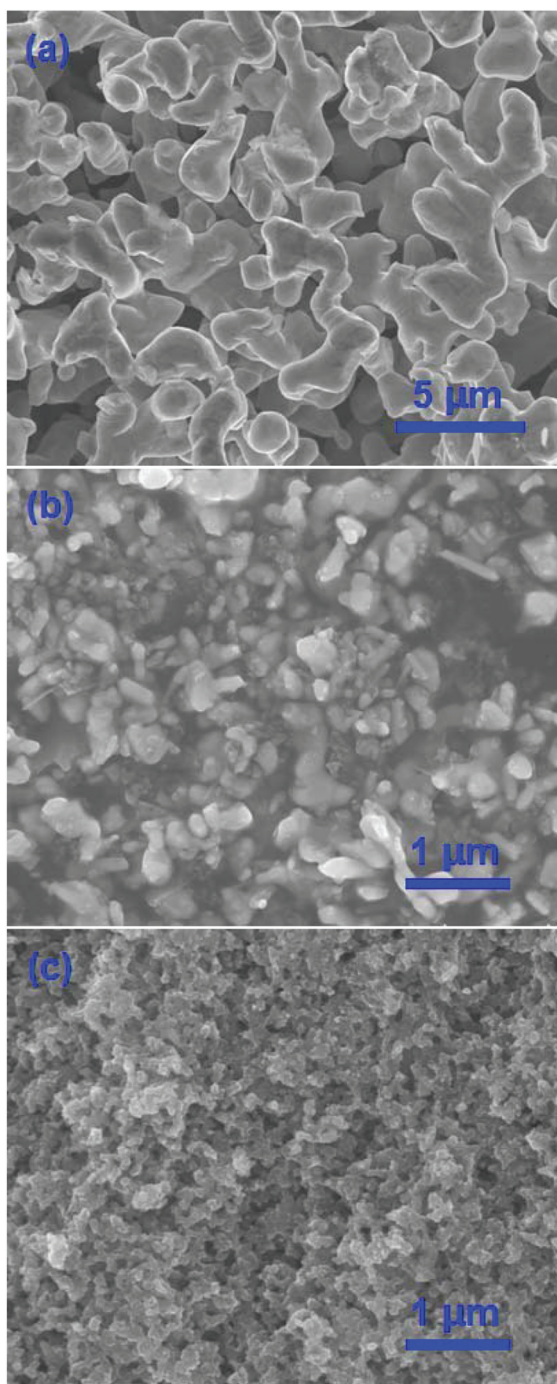


Fig. 3 SEM images of (a) S-Ni₂P, (b) S-Co₂P and (c) S-MoP.

3.2 Formation pathway of phosphides

To give insights into the formation process of phosphides obtained from mixtures of NiO/P₂O₅, Co₃O₄/P₂O₅ and MoO₃/P₂O₅, some intermediate samples were characterized by XRD. In view of the fact that the temperature-dependent reduction process usually involved simultaneously two aspects (heat-treatment and reduction), the treatments of these mixture precursors in the absence/presence of H₂ should be investigated. In addition, for the sake of comparison, the phase structures

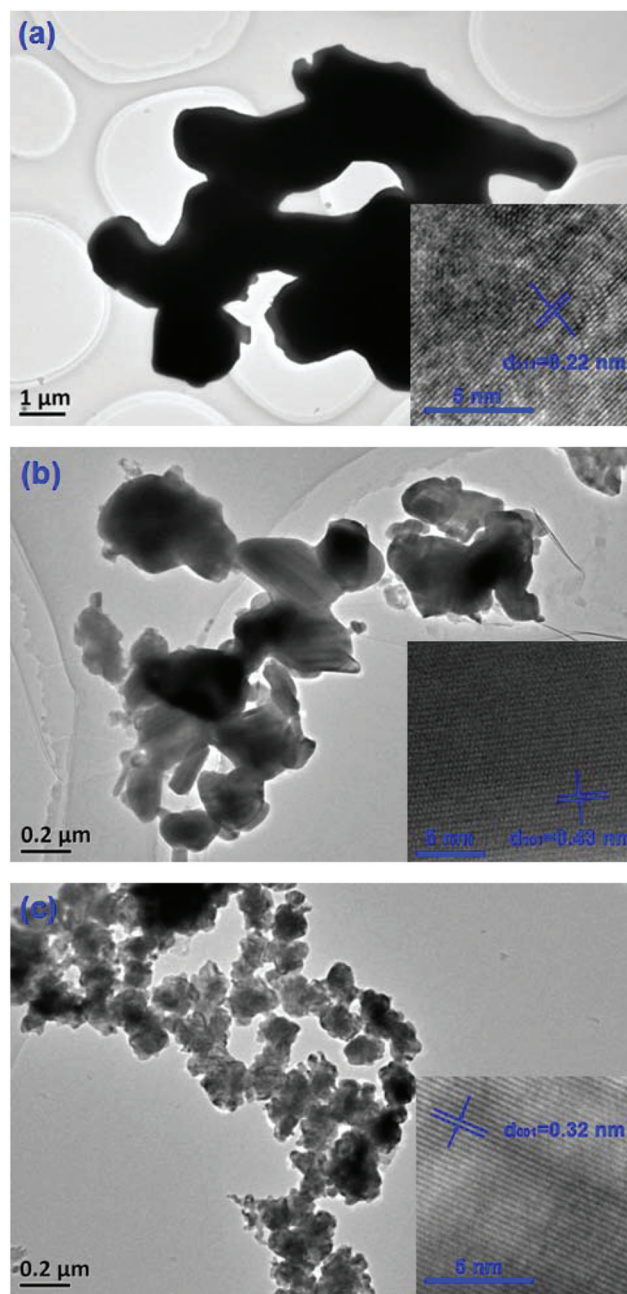
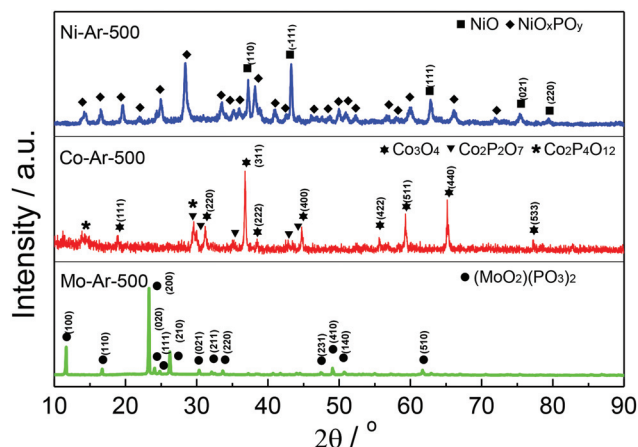


Fig. 4 Low and high resolution TEM images of (a) S-Ni₂P, (b) S-Co₂P and (c) S-MoP.

of the products obtained in the study are listed in Table 3. Fig. 5 shows the XRD patterns of the solid mixture precursors treated at 500 °C in the absence of H₂. After heating these solid mixtures at 500 °C in Ar, Co₃O₄ and MoO₃ can react with P₂O₅ to produce cobalt phosphates (Co₂P₂O₇ (main peaks at 2θ of 29.6°, 30.1° and 35.2°) and Co₂P₄O₁₂ (main peaks at 2θ of 14.3° and 29.6°)) and (MoO₂)(PO₃)₂ (main peaks at 2θ of 11.5°, 16.6°, 23.1°, 24.0° and 26.2°, corresponding to the (100), (110), (200), (020) and (210) planes). In the case of NiO/P₂O₅, a set of peaks marked with rhombuses were found, but they cannot be assigned to any (known) Ni oxides, Ni phosphates or Ni oxide-

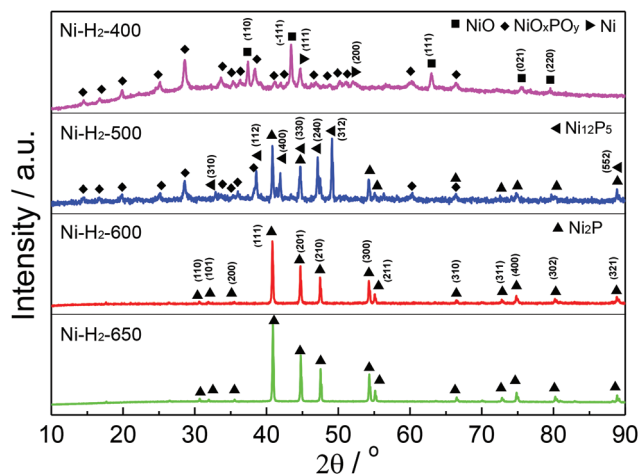
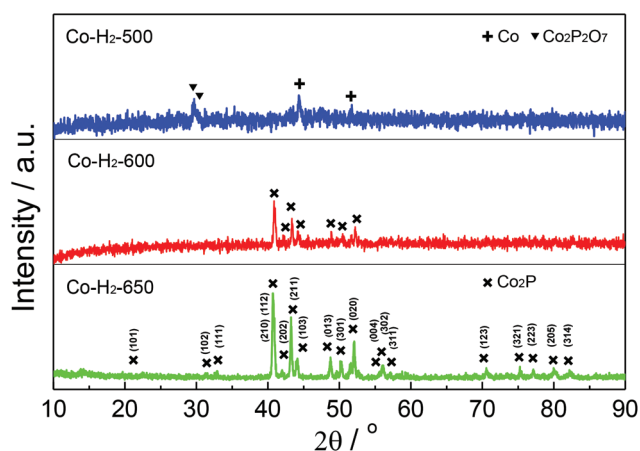
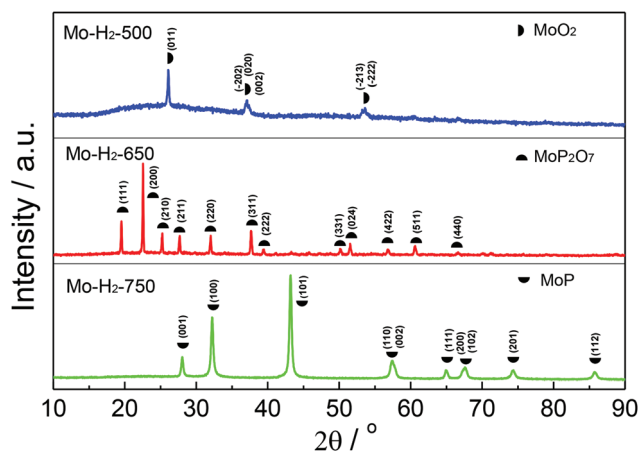
Table 3 Phase structures of the samples obtained in this study

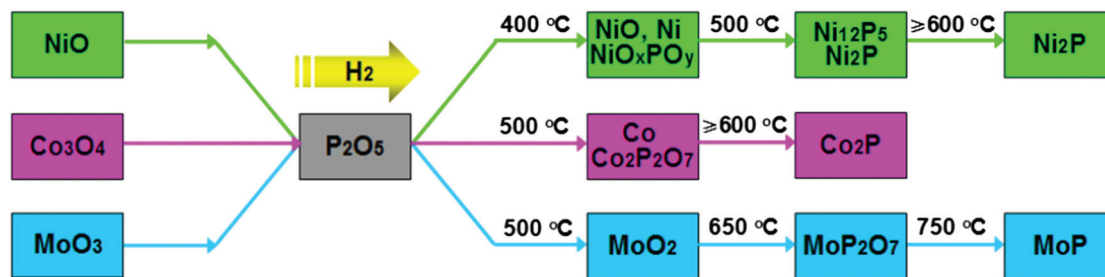
Sample	XRD phases	JCPDS cards
Ni-Ar-500	NiO, NiO _x PO _y	89-7131, —
Co-Ar-500	Co ₃ O ₄ , Co ₂ P ₂ O ₇ , Co ₂ P ₄ O ₁₂	09-0418, 49-1091, 40-0068
Mo-Ar-500	(MoO ₂)(PO ₃) ₂	74-1389
Ni-H ₂ -400	NiO, Ni, NiO _x PO _y	89-7131, 65-0380, —
Ni-H ₂ -500	Ni ₁₂ P ₅ , Ni ₂ P	74-1381, 65-1989
Ni-H ₂ -600	Ni ₂ P	65-1989
Ni-H ₂ -650	Ni ₂ P	65-1989
Co-H ₂ -500	Co, Co ₂ P ₂ O ₇	15-0806, 49-1091
Co-H ₂ -600	Co ₂ P	65-2380
Co-H ₂ -650	Co ₂ P	65-2380
Mo-H ₂ -500	MoO ₂	78-1069
Mo-H ₂ -650	MoP ₂ O ₇	84-1794
Mo-H ₂ -750	MoP	65-6487

**Fig. 5** XRD patterns of the mixture precursors (NiO/P₂O₅, Co₃O₄/P₂O₅ and MoO₃/P₂O₅) treated at 500 °C in Ar.

phosphates. Thus, it can be inferred from the XRD that NiO can react with P₂O₅ to yield an unknown compound (NiO_xPO_y). These results indicated that all the above mentioned MOs can be transformed into metal phosphates or metal oxide-phosphates when the solid mixtures were heated in the absence of H₂. However, the absence of diffraction peaks of phosphorus oxides in Fig. 5 was probably due to their amorphous forms or high dispersion on the solid surface.^{50,51}

Fig. 6–8 shows the XRD patterns of the solid mixture precursors treated at different temperatures in a H₂ atmosphere. In the case of the NiO/P₂O₅ sample, it can be observed from Fig. 6 that at 400 °C, the precursor was transformed into a mixture of NiO, NiO_xPO_y and Ni metal (main peaks at 2θ of 44.3 and 51.7, indexed to the (111) and (200) planes, respectively). The result indicated that a portion of NiO was reduced by H₂ to Ni; however, it interacted with P₂O₅ to produce NiO_xPO_y during heat-treatment process (see Fig. 5). When the temperature was increased to 500 °C, the peaks for NiO, Ni and NiO_xPO_y disappeared or weakened, and there were new peaks corresponded to Ni₁₂P₅ (main peaks at 2θ of 32.7°, 38.4°, 41.8°, 47.0° and 49.0°, indexed to (310), (112), (400), (240) and (312) planes, respectively) and Ni₂P (main peaks at

**Fig. 6** XRD patterns of the NiO/P₂O₅ precursor for Ni₂P treated at different temperatures in H₂ flow.**Fig. 7** XRD patterns of the Co₃O₄/P₂O₅ precursor for Co₂P treated at different temperatures in H₂ flow.**Fig. 8** XRD patterns of the MoO₃/P₂O₅ precursor for MoP treated at different temperatures in H₂ flow.



Scheme 1 Schematic of the phases formed during reduction of the MOs/P₂O₅ precursors.

2θ of 40.7°, 44.6°, 47.4°, 54.2° and 55.0°, due to the (111), (201), (210), (300) and (211) planes, respectively) phases. With a further increase in temperature (≥ 600 °C), all the Ni-containing species were converted to Ni phosphides in H₂ flow and there was a clear phase transformation (Ni₁₂P₅ → Ni₂P) in the sample just as the observation reported before,^{35,36} and then phase-pure Ni₂P can be obtained as a final product.

In the case of Co₃O₄/P₂O₅ sample (Fig. 7), a mixture of Co metal (main peaks at 2θ of 44.4° and 51.6°) and Co₂P₂O₇ (main peaks at 2θ of 29.6° and 30.1°) was obtained after heating the precursor at 500 °C in H₂, indicating that a portion of Co₃O₄ was reduced to Co metal, and the rest was transformed into cobalt phosphate (Co₂P₂O₇) due to its reactivity with P₂O₅ (see Fig. 5). When the temperature was increased to 600 °C, those Co-containing species obtained at 500 °C were completely converted to the desired product Co₂P. The intensity of the Co₂P peaks increased with temperature, and the well crystalline Co₂P (main peaks at 2θ of 40.7°, 41.0°, 42.1°, 43.3°, 44.1°, 48.7°, 50.4°, 52.0° and 56.2°, indexed to the (112), (210), (202), (211), (103), (013), (301), (020) and (302) planes, respectively) can be obtained at 650 °C.

As for the MoO₃/P₂O₅ sample (see Fig. 8), it was clear that the diffraction peaks for MoO₂ (main peaks at 2θ of 26.0°, 36.7°, 37.0°, 37.2°, 53.0° and 53.1°, indexed to the (011), (−202), (020), (002), (−213) and (−222) planes, respectively) can be observed when the sample was heated at 500 °C in H₂ flow, but there were no peaks for the (MoO₂)(PO₃)₂ phase mentioned above in Fig. 5, indicating that MoO₃ was preferentially converted to low-valence Mo oxide rather than Mo oxide-phosphate at 500 °C in the presence of H₂. With an increase of the temperature to 650 °C, no reflections for Mo phosphide were found. However, conversely, MoO₂ was transformed into MoP₂O₇ (main peaks at 2θ of 19.3°, 22.4°, 25.0°, 27.5°, 31.8° and 37.5°, corresponding to the (111), (200), (210), (211), (220) and (311) planes) instead of being further reduced to Mo metal because the reduction of MoO₂ required a higher temperature (>700 °C).⁵² Fortunately, when the temperature was further increased to 750 °C, the peaks for MoP₂O₇ disappeared, and main diffraction peaks at 28.0°, 32.1°, 43.1°, 57.3°, 64.9°, 67.6°, 74.2° and 85.7° were observed, corresponding to the (001), (100), (101), (110)/(002), (111), (200)/(102), (201) and (112) planes of MoP.

In addition, the background features to the XRD patterns (Fig. 6–8), especially for those of Ni–H₂-400 and Mo–H₂-500, appeared consistent with some amorphous components. Some phosphorus oxides and metal (metal–oxide) phosphates were reported to be amorphous and were usually involved in the traditional precursors for the synthesis of phosphides *via* the H₂-TPR method,^{6,50,51} thus it was reasonable to deduce that in the present study the reactions between P₂O₅ and metal oxides might also yield a small amount of these amorphous phases. However, at higher temperatures (≥ 650 °C), the amorphous metal (metal–oxide) phosphate phases and amorphous phosphorus oxide/metal oxide mixtures were easily reduced by H₂ to produce metal phosphides,⁶ which agreed with the XRD results that the amorphous backgrounds disappeared on the XRD patterns of Ni–H₂-650, Co–H₂-650 and Mo–H₂-750. Moreover, the clear lattice fringes in the HRTEM images (Fig. 4) further confirmed the high crystalline nature of the synthesized metal phosphides.

The syntheses utilized in this study to prepare metal phosphides involved mixing of MOs and P₂O₅ and subsequent reduction with H₂. Based on the results of XRD, XPS, SEM and TEM, the investigation of the synthesis processes (see Scheme 1) clearly showed that MOs can be reduced at relatively low temperatures to corresponding metals or low-valence oxides, at the same time, MOs can also be reacted with P₂O₅ to form metal phosphates or metal oxide-phosphates. A small portion of these phosphates still remained amorphous. Finally, these metal-containing species (metal oxides, metals, metal phosphates and metal oxide-phosphates) were converted to metal phosphides at relatively high temperatures. The formation pathway of phosphides using MOs/P₂O₅ mixtures as precursors can be clarified as MOs/P₂O₅ precursors → complex intermediates (metals, metal phosphates and metal oxide-phosphates) → metal phosphides.

The route presented showed a number of advantages in comparison to the traditional H₂-TPR method using (NH₄)₂HPO₄ and metal salts as starting materials. The precursors used in the route were obtained simply by mechanical mixing of metal oxides (MOs) and P₂O₅, instead of dissolution, drying and calcination steps involved in the preparation procedure for traditional precursors; the route favored the formation of phosphides *via* various specific intermediates,

which can be helpful to understand the formation mechanism; the dispersions of the phosphides obtained from MOs/P₂O₅ precursors were superior to those of phosphides prepared from the traditional precursors. Finally, it was suggested that the route might be feasible for large scale preparation of phosphides and this aspect will be investigated in the future.

4. Conclusions

In summary, we developed a new MOs/P₂O₅ precursors for the synthesis of Ni₂P, Co₂P and MoP phosphides *via* the H₂ reduction method. Compared with the traditional precursors obtained from metal salts and (NH₄)₂HPO₄ *via* dissolution, drying and calcination, this new type of precursor was prepared only by simple mechanical mixing of starting materials. Furthermore, the formation pathway of phosphides using the precursors can be proposed as the MOs/P₂O₅ precursors shifting to the phosphide products *via* metal, metal phosphate and metal oxide-phosphate intermediates. In addition, it was found that the dispersions of Ni₂P, Co₂P and MoP obtained from MOs/P₂O₅ precursors were superior to those of the corresponding phosphides prepared from the traditional precursors. This was because the morphology of as-prepared metal phosphides might be inherited from corresponding MOs.

Acknowledgements

We acknowledge the financial support from the National Natural Science Foundation of China (No. 21276253).

Notes and references

- 1 A.-M. Alexander and J. S. J. Hargreaves, *Chem. Soc. Rev.*, 2010, **39**, 4388–4401.
- 2 E. J. Popczun, J. R. McKone, C. G. Read, A. J. Biacchi, A. M. Wiltrout, N. S. Lewis and R. E. Schaak, *J. Am. Chem. Soc.*, 2013, **135**, 9267–9270.
- 3 K. Y. Yoon, Y. Jang, J. Park, Y. Hwang, B. Koo, J.-G. Park and T. Hyeon, *J. Solid State Chem.*, 2008, **181**, 1609–1613.
- 4 X. C. Jiang, Q. H. Xiong, S. Nam, F. Qian, Y. Li and C. M. Lieber, *Nano Lett.*, 2007, **7**, 3214–3218.
- 5 C. Stinner, R. Prins and Th. Weber, *J. Catal.*, 2000, **191**, 438–444.
- 6 X. Wang, P. Clark and S. T. Oyama, *J. Catal.*, 2002, **208**, 321–331.
- 7 Q. Guan and W. Li, *J. Catal.*, 2010, **271**, 413–415.
- 8 J. A. Cecilia, A. Infantes-Molina, E. Rodríguez-Castellón and A. Jiménez-López, *Appl. Catal., B*, 2009, **92**, 100–113.
- 9 E. J. Popczun, C. G. Read, C. W. Roske, N. S. Lewis and R. E. Schaak, *Angew. Chem., Int. Ed.*, 2014, **126**, 5531–5534.
- 10 L. Feng, H. Vruble, M. Bensimon and X. Hu, *Phys. Chem. Chem. Phys.*, 2014, **16**, 5917–5921.
- 11 L. Ding, Y. Shu, A. Wang, M. Zheng, L. Li, X. Wang and T. Zhang, *Appl. Catal., A*, 2010, **385**, 232–237.
- 12 R. Cheng, Y. Shu, M. Zheng, L. Li, J. Sun, X. Wang and T. Zhang, *J. Catal.*, 2007, **249**, 397–400.
- 13 M. Zheng, Y. Shu, J. Sun and T. Zhang, *Catal. Lett.*, 2008, **121**, 90–96.
- 14 Z. W. Yao, H. Dong and Y. Shang, *J. Alloys. Compd.*, 2009, **474**, L10–L13.
- 15 S. T. Oyama, *J. Catal.*, 2003, **216**, 343–352.
- 16 R. Cheng, Y. Shu, M. Zheng, L. Li, J. Sun, X. Wang and T. Zhang, *J. Catal.*, 2007, **249**, 397–400.
- 17 S. Carenco, D. Portehault, C. Boissière, N. Mézailles and C. Sanchez, *Chem. Rev.*, 2013, **113**, 7981–8065.
- 18 A. Wang, M. Qin, J. Guan, L. Wang, H. Guo, X. Li, Y. Wang and R. Prins, *Angew. Chem., Int. Ed.*, 2008, **120**, 6141–6143.
- 19 J. Guan, Y. Wang, M. Qin, Y. Yang, X. Li and A. Wang, *J. Solid State Chem.*, 2009, **182**, 1550–1555.
- 20 S. Yang, C. Liang and R. Prins, *J. Catal.*, 2006, **237**, 118–130.
- 21 Y. Xie, H. L. Su, X. F. Qian, X. M. Liu and Y. T. Qian, *J. Solid State Chem.*, 2000, **149**, 88–91.
- 22 Y. Ni, L. Jin and J. Hong, *Nanoscale*, 2011, **3**, 196–200.
- 23 J. Park, B. Koo, K. Y. Yoon, Y. Hwang, M. Kang, J.-G. Park and T. Hyeon, *J. Am. Chem. Soc.*, 2005, **127**, 8433–8440.
- 24 A. E. Henkes and R. E. Schaak, *Chem. Mater.*, 2007, **19**, 4234–4242.
- 25 E. Muthuswamy, G. H. L. Savithra and S. L. Brock, *ACS Nano*, 2011, **5**, 2402–2411.
- 26 L. Li and P. Reiss, *J. Am. Chem. Soc.*, 2008, **130**, 11588–11589.
- 27 W.-S. Ojo, S. Xu, F. Delpech, C. Nayral and B. Chaudret, *Angew. Chem., Int. Ed.*, 2012, **51**, 738–741.
- 28 W. Maneepprakorn, C. Q. Nguyen, M. A. Malik, P. O'Brien and J. Raftery, *Dalton Trans.*, 2009, 2103–2108.
- 29 S. Liu, X. Liu, L. Xu, Y. Qian and X. Ma, *J. Cryst. Growth*, 2007, **304**, 430–434.
- 30 X. Hu and J. C. Yu, *Chem. Mater.*, 2008, **20**, 6743–6749.
- 31 A. Panneerselvam, M. A. Malik, M. Afzaal, P. O'Brien and M. Helliwell, *J. Am. Chem. Soc.*, 2008, **130**, 2420–2421.
- 32 X. Wang, P. Clark and S. T. Oyama, *J. Catal.*, 2002, **208**, 321–331.
- 33 I. I. Abu and K. J. Smith, *J. Catal.*, 2006, **241**, 356–366.
- 34 V. Zuzaniuk and R. Prins, *J. Catal.*, 2003, **219**, 85–96.
- 35 Z. Yao, G. Wang, Y. Shi, Y. Zhao, J. Jiang, Y. Zhang and H. Wang, *Dalton Trans.*, 2015, **44**, 14122–14129.
- 36 Z. Yao, M. Li, X. Wang, X. Qiao, J. Zhu, Y. Zhao, G. Wang, J. Yin and H. Wang, *Dalton Trans.*, 2015, **44**, 5503–5509.
- 37 A. W. Burns, A. F. Gaudette and M. E. Bussell, *J. Catal.*, 2008, **260**, 262–269.
- 38 Q. Guan, X. Cheng, R. Li and W. Li, *J. Catal.*, 2013, **299**, 1–9.
- 39 S. S.-Y. Lin, D. H. Kim, M. H. Engelhard and S. Y. Ha, *J. Catal.*, 2010, **273**, 229–235.
- 40 J. Chen, H. Shi, L. Li and K. Li, *Appl. Catal., B*, 2014, **144**, 870–884.

- 41 R. Heuberger, A. Rossi and N. D. Spencer, *Tribol. Lett.*, 2007, **25**, 185–196.
- 42 Z. Qi and W. Lee, *Tribol. Int.*, 2010, **43**, 810–814.
- 43 S. Survilienė, V. Jasulaitienė, A. Češūnienė and A. Lisowska-Oleksiak, *Solid State Ionics*, 2008, **179**, 222–227.
- 44 J. A. Schaidle, A. C. Lausche and L. T. Thompson, *J. Catal.*, 2010, **272**, 235–245.
- 45 P. Xiao, M. A. Sk, L. Thia, X. Ge, R. J. Lim, J.-Y. Wang, K. H. Lim and X. Wang, *Energy Environ. Sci.*, 2014, **7**, 2624–2629.
- 46 V. M. L. Whiffen, K. J. Smith and S. K. Straus, *Appl. Catal., A*, 2012, **419–420**, 111–125.
- 47 R. Cheng, Y. Shu, L. Li, M. Zheng, X. Wang, A. Wang and T. Zhang, *Appl. Catal., A*, 2007, **316**, 160–168.
- 48 Q. Guan and W. Li, *J. Catal.*, 2010, **271**, 413–415.
- 49 Z. Yao, H. Hai, Z. Lai, X. Zhang, F. Peng and C. Yan, *Top. Catal.*, 2012, **55**, 1040–1045.
- 50 Z. Yao, Z. Lai, X. Zhang, F. Peng, H. Yu and H. Wang, *Mater. Res. Bull.*, 2011, **46**, 1938–1941.
- 51 Y. Teng, A. Wang, X. Li, J. Xie, Y. Wang and Y. Hu, *J. Catal.*, 2009, **266**, 369–379.
- 52 C. Shi, A. M. Zhu, X. F. Yang and C. T. Au, *Appl. Catal., A*, 2004, **276**, 223–230.